A Novel Fast Otsu Digital Image Segmentation Method

Duaa AlSaeed[1, 2], Ahmed Bouridane[1, 2], and Ali El-Zaart[3]
[1]Department of Computer Science and Digital Technologies, Northumbria University at Newcastle, UK
[2]College of Computer and Information Sciences, King Saud University, Saudi Arabia
[3]Department of Computer Science, Beirut Arab University, Lebanon

Abstract: *Digital image segmentation based on Otsu's method is one of the most widely used technique for threshold selection. With Otsu's method, an optimum threshold is found by maximizing the between-class variance and the algorithm assumes that the image contains two classes of pixels or bi-modal histogram (e.g., foreground and background). It then calculates the optimal threshold value separating these two classes so that, their between class variance is maximal. The optimum threshold value is found by an exhaustive search among the full range of gray levels (e.g., 256 levels of intensity). The objective of this paper is to develop a fast algorithm for the Otsu method that reduces the number of search iterations. A new search technique is developed and compared with the original Otsu method. Experiments on several images show that the proposed Otsu-Checkpoints fast method give the same estimated threshold value with less number of iterations thus resulting in a much less computational complexity.*

Keywords: *Image thresholding, otsu method, optimized search technique.*

Received April 23, 2013; accepted June 23, 2014; published online August 22, 2015

1. Introduction

Digital image segmentation is a fundamental step in many image analysis applications and is a very critical task. One can define image segmentation as a partitioning or clustering technique used for image analysis. In another words, it is a process of subdividing an image into its constituent regions or objects as part of the analysis process [4, 7, 15]. Image segmentation algorithms are generally based on one of two basic properties of intensity values: Discontinuity and similarity. In the first type, an image is partitioned based on sudden changes in intensity (e.g., gray level), while in the other type, an image is partitioned into regions that are considered to be similar based on certain criteria [7, 15]. Otsu method is one of the well-known thresholding methods and involves an iterating process through all the possible threshold values and calculating a measure of spread for the pixel levels each side of the threshold, i.e., the pixels that fall in either foreground or background. The aim is to determine the threshold value where the sum of the foreground and background spreads is at its minimum since the threshold value having a maximum between-class variance has also a minimum within-class variance. Therefore, it is a good alternative to use the between-class variance for finding optimum threshold since it requires less computational complexity [15, 16, 18]. In addition, there does not exist a single image segmentation algorithm, which can give the best result for every digital image. Depending on to the type of the given image application the most appropriate approach is to be chosen to achieve the best segmentation result. In some applications, the processing time (or computational complexity) is an essential issue. For example, in biometric authentication and verification systems this is a typical constraint in addition to an efficient segmentation.

The method proposed in this paper is aimed to develop a faster method for estimating the optimal threshold value in Otsu method by minimizing the number of search iterations along possible threshold values. This is achieved by selecting a sub-range of gray levels around an initial estimated threshold value while still keeping the keeping the quality of the segmentation process intact.

The paper is organized as follows: Section 2 introduces the segmentation process in general and thresholding technique in particular. Section 3 presents a brief introduction on Otsu method of thresholding. The proposed technique is explained in section 4 while section 5 is concerned with the experimental results carried out. Section 6 concludes the paper.

2. Image Thresholding

Digital image segmentation has been a major research topic in digital image processing resulting a variety of methods and algorithms developed and improved for image segmentation ranging from general segmentation methods to tailored for certain image type or a certain application [2, 17]. Each method has a different approach in defining what characterizes a good segmentation and uses a different technique to find the optimal segmentation [13, 14]. Image thresholding is one of the main approaches of segmentation and Otsu thresholding method is one well-known thresholding technique.

Image thresholding is considered the easiest way to segment an image. Although, it seems simple the problem of choosing a good and an accurate threshold value is a difficult task. Thresholding is most commonly used for separating objects from the background [3, 9, 10, 11, 15]. The most widely used thresholding technique uses the gray level histogram. When an image, $f(x, y)$ is composed of dark objects on a light background, then the foreground is clearly distinguishable from the background. In this case, the image histogram will be bimodal so that, the threshold value will lie in the valley of the histogram ensuring that the objects can be extracted by comparing pixel values with a threshold T. If any pixel (x, y) for which $f(x, y)\geq T$ is considered as belonging to the object class, otherwise, it belongs to the background class [7, 8]. Unfortunately, this is not the case in most images. In addition to histogram based thresholding techniques, several techniques have been proposed, trying to find a way of choosing the best value of threshold T that will result in an accurate segmentation. Otsu method is one of the widely used thresholding methods; Otsu's method involves iterating through all possible threshold values and calculating the weighted sum of within-class variances of the foreground and background pixels. The aim is to find the threshold value where the sum of within-class variances is at its minimum.

3. The Otsu's Method

Let the pixels of a given picture be represented in L gray levels [1, 2, ..., L]. The number of pixels at level i is denoted by n_i and the total number of pixels by $N=n_1+n_2+...+n_L$. The probability distribution [8, 12, 16]:

$$p_i=\frac{n_i}{N},\ p_i\geq 0, \Sigma_{i=1}^{L} p_i=1 \tag{1}$$

Now, when we classify the pixels into two classes C_0 and C_1 (background and objects) by a threshold at level t, C_0 denotes pixels with gray levels [1, 2, ..., t] and C_1 denotes pixels with levels [t+1, ..., L]. Then, the probability of class occurrence and class mean respectively are [1, 12]:

$$\omega_0= p_r(C_0)=\sum_{i=1}^{t} p_i=\omega(t) \tag{2}$$

$$\omega_1= p_r(C_1)=\sum_{i=t+1}^{L} p_i=-\omega(t) \tag{3}$$

And

$$\mu_0=\sum_{i=1}^{t} ip_r(i\setminus C_0)=\sum_{i=1}^{t} i\frac{p_i}{\omega_0}=\frac{\mu(t)}{\omega(t)} \tag{4}$$

$$\mu_1=\sum_{i=t+1}^{L} ip_r(i\setminus C_1)=\sum_{i=t+1}^{L}\frac{p_r}{\omega_1}=\frac{\mu_T-\mu(\mathrm{t})}{1-\omega(\mathrm{t})} \tag{5}$$

Where ω_t and μ_t are the 0^{th} and 1^{st} order cumulative moments of the histogram up to t^{th} level and are defined as follow:

$$\omega(t)=\sum_{i=1}^{t} p_i \tag{6}$$

And

$$\mu(t)=\sum_{i=1}^{t} ip_i \tag{7}$$

And μ_t is the total mean level of the original image which is computed as:

$$\mu_T=\mu(L)=\sum_{i=1}^{t} ip_i \tag{8}$$

For any t; the following relation is valid:

$$\mu_0\omega_0+\mu_1\omega_1=\mu_\mathrm{T},\ \omega_0+\omega_1=1 \tag{9}$$

The class variances and total variance are given by:

$$\sigma_0^2=\sum_{i=1}^{t}(i-\mu_0)^2 p_r(i\setminus C_0)=\sum_{i=1}^{t}(i-\mu_0)^2\frac{p_i}{\omega_0} \tag{10}$$

$$\sigma_1^2=\sum_{i=t+1}^{L}(i-\mu_1)^2 p_r(i\setminus C_1)=\sum_{i=t+1}^{L}(i-\mu_1)^2\frac{p_i}{\omega_1} \tag{11}$$

In order to evaluate the goodness of the threshold (at level t), within-class variance and between-class variance are used as measures of class separability. They are are defined, respectively as follows:

$$\sigma_W^2=\omega_0\sigma_0^2+\omega_1\sigma_1^2 \tag{12}$$

$$\sigma_B^2=\omega_0(\mu_0-\mu_T)^2+\omega_1(\mu_1-\mu_T)^2=\omega_0\omega_1(\mu_1-\mu_0)^2 \tag{13}$$

And the following relations hold:

$$\eta=\frac{\sigma_B^2}{\sigma_T^2} \tag{14}$$

$$\sigma_T^2=\sigma_B^2+\sigma_W^2 \tag{15}$$

The problem is then reduced to maximize one of these criterion measures. It is noticed that σ_B^2 is dependent on 1^{st} order statistics while σ_W^2 depends on the 2^{nd} order statistics. Therefore, σ_B^2 is the simplest measure with respect to t. Thus, $\eta(t)$ is adopted as the criterion measure to select the best threshold value (t) which is determined by a sequential search by using the following functions [12]:

$$\eta(\mathrm{t})=\frac{\sigma_B^2(\mathrm{t})}{\sigma_T^2} \tag{16}$$

$$\sigma_B^2(\mathrm{t})=\frac{[\mu_T\,\omega(\mathrm{t})-\mu(\mathrm{t})]^2}{\omega(t)\left[1-\omega(\mathrm{t})\right]} \tag{17}$$

Since, σ_T^2 is not a function of threshold (t), then the optimal threshold should be the value which maximizes $\sigma_B^2(t)$. Thus the optimal value threshold (t^*) is computed with the following equation [12]:

$$\sigma_B^2(t^*)=max\,\sigma_B^2(t), 1\leq t<L \tag{18}$$

4. Proposed New Fast-Otsu Methods (Otsu-Checkpoints)

In Otsu method the value of $\sigma_B^2(t)$ is computed for each t, $0 \leq t \leq L$. Once this done, the minimal value of $\sigma_B^2(t)$, say $\sigma_B^2(t^*)$ is selected from these L values and t^* is then considered as the optimal threshold value [12]. By using Equation 18, for each t the computational effort for calculating $\sigma_B^2(t)$ is bounded by cL, where c is constant. By considering the time complexity notation [6], let $f(t)$ be the time complexity for t to calculate $\sigma_B^2(t)$, therefore, $f(t) \leq cL$, i.e., $f(t)=O(L)$. For $0 \leq t \leq L$, it requires $O(L^2)$ cycles to calculate all $\sigma_B^2(t)^s$ [5]. Our aim is to speed up the process of Otsu thresholding by developing a fast iterative Otsu thresholding algorithm. We speed up the process by iteratively minimizing the range of possible threshold values until the range reaches its minimum length, which is 3 gray level.

For a bimodal histogram, in most of the cases the optimal threshold estimated by Otsu method should not be far from image global mean mu_T. Figures 1 and 2 show examples of an image and its histogram. Considering this, we can narrow the search range to a certain distance around the local mean. However, since this is not the case in all images, instead of building the search range only around the global mean; we propose to set our initial search range to the full gray level range. In that range we then set three checkpoints, choose the one with the maximum Between Class Variance (BCV) σ_B^2, then set it as the initial estimated threshold T_{init}. Around this estimated threshold value, we will build the new search range and repeat the same process of setting checkpoints and narrowing the search range until we reach one of our stopping conditions:

1. The BCV at the selected initial threshold T_{init} has BCV larger than the two gray levels around it (T_{init}-1, T_{init}+1), in this case we will set optimal threshold to T_{init} and exit our search process.
2. The range become only three gray levels length, at this point we will set the optimal threshold to the one of the 3 gray levels that has the maximum between class variance BCV and exit our search process.

Figure 3 depicts an example of an image and its histogram showing the phases of our search process.

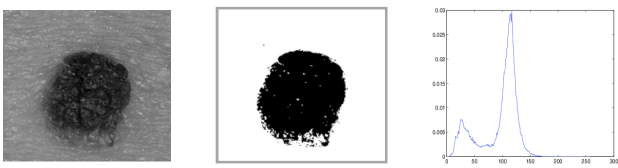

a) Original. b) Otsu-T=91. c) Histogram.

Figure 1. Original, histogram and segmented image of skin cancer 5.

a) Original. b) Otsu-T=90. c) Histogram.

Figure 2. Original, histogram and segmented image of einstein.

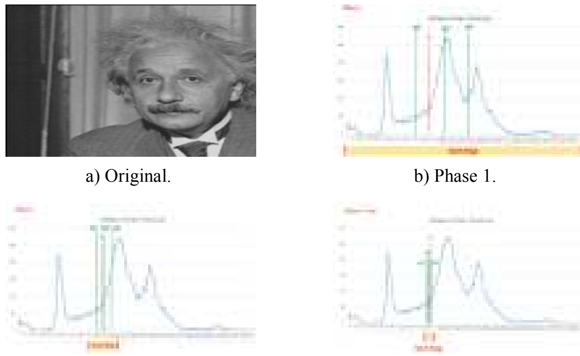

a) Original. b) Phase 1. c) Phase 2. d) Phase 3.

Figure 3. Original image and stages for finding optimal threshold for image of einstein.

Now, in our initial stage we set the initial check points to the global mean of the full histogram as the mid-checkpoint icp_2 and two local means of the two parts of the histogram after splitting it into two parts on each side of this mid-checkpoint. This results in 3 initial checkpoints (icp_1, icp_2, icp_3) for which we compute ($\sigma_B^2(icp_1)$, $\sigma_B^2(icp_2)$, $\sigma_B^2(icp_3)$), respectively. The three initial checkpoints are defined, respectively as:

$$icp_2 = \mu_T = \sum_{j=1}^{L} jp_j \tag{19}$$

$$icp_1 = \sum_{j=1}^{icp_2} jp_j \tag{20}$$

$$icp_3 = \sum_{j=icp_2+1}^{L} jp_j \tag{21}$$

These check points divide the image histogram of an image, $f(x, y)$ into four initial sub-ranges, as follows:

$$iRange_1 = min(f(x, y)), \ldots, icp_1 \tag{22}$$

$$iRange_2 = icp_1, \ldots, icp_2 \tag{23}$$

$$iRange_3 = icp_2, \ldots, icp_3 \tag{24}$$

$$iRange_4 = icp_3, \ldots, max(f(x, y)) \tag{25}$$

In our proposed optimized search techniques, we will choose the checkpoint with the maximum $\sigma_B^2(t)$ and set it as the initial estimated threshold T_{init}. Next, we will narrow the search range for the next stage to one of the two initial sub-ranges bounded by this checkpoint (initial estimated threshold T_{init}). To select the sub-range, we will do the following:

1. Check BCV for the two gray levels around it (T_{init}-1,

T_{init}+1) and compare it to BCV at this checkpoint.
2. If max BCV is at (T_{init}-1) we select the sub-range that ends at this checkpoint.
3. If (T_{init}+1) has max BCV, we select the sub-range that starts at this checkpoint.
4. On the other hand, if T_{init} itself has max BCV, we then will stop our search process and set the optimal threshold to T_{init}.

Now, in the following stages and in case we didn't exit the search process, we will set our checkpoints differently. For the current sub-range R_c=[r_1, r_2], the three check points (cp_1, cp_2, cp_3) are set as follows:

$$cp_2 = r_1 + \frac{(r_2 - r_1)}{2} \quad (26)$$

$$cp_1 = r_1 + \frac{cp_2 - r_1}{2} \quad (27)$$

$$cp_3 = cp_1 + \frac{r_2 - cp_2}{2} \quad (28)$$

These check points will again divide the current histogram range into four new sub-ranges, as follows:

$$Range_1 = r_1, \dots, cp_1 \quad (29)$$

$$Range_2 = cp_1, \dots, cp_2 \quad (30)$$

$$Range_3 = cp_2, \dots, cp_3 \quad (31)$$

$$Range_4 = cp_3, \dots, r_2 \quad (32)$$

Once again, we will choose the checkpoint with the maximum $\sigma_B^2(t)$, then we narrow the search range in the same way done in the initial stage; This process will keep repeated until the optimal threshold is found or the selected sub-range is small enough that is when the range is made of only 3 gray levels.

The proposed search algorithm can be summarized in the following steps:

1. Compute image histogram $hist(f(x, y))$ and probabilities of each intensity level $Prop(f(x, y))$.
2. Find icp_2, P_1 and icp_3 using Equations 19, 20, 21 respectively.
3. Compute ($\sigma_B^2(icp_1)$, $\sigma_B^2(icp_2)$, $\sigma_B^2(icp_3)$), using Equation 17.
4. Find $Max_{j=1:3}(\sigma_B^2(icp_j))$.
5. Set initial threshold T_{init} equals to selected checkpoint icp_j.
6. Using one of the ranges defined in Equations 22, 23, 24, 25 set next search range R_c=[r_1, r_2] as follows:
   a. Check BCV for the two gray levels around it (T_{init}-1, T_{init}+1) and compare it to BCV at this checkpoint.
   b. If max BCV is at (T_{init}-1) we select the sub-range that ends at this checkpoint.
   c. If has max BCV, we select the sub-range that starts at this checkpoint.
   d. On the other hand, if T_{init} has max BCV, then optimal threshold t^* is found and set to T_{init} and we stop our search process.
7. While (size(Sub-range)> 3) and (optimal threshold is not found) do:
   a. Find P_2, cp_1 and cp_3 using Equations 26, 27, 28 respectively.
   b. Compute ($\sigma_B^2(cp_1)$, $\sigma_B^2(cp_2)$, $\sigma_B^2(cp_3)$), using Equation 17.
   c. $Max_{j=1:3}(\sigma_B^2(cp_j))$.
   d. Using one of the ranges defined in Equations 29, 30, 31 and 32, we check and set next search range R_c=[r_1, r_2] in the same manner described in step 6.
8. If size(Sub-range)= 3, then $\forall t$™ current sub-range R_c, Compute $\sigma_B^2(t)$, using Equation 18.
9. Set optimal threshold t^* to t with $Max\sigma_B^2(t)$.

Table 1 compares the pseudo code and performance for original Otsu and proposed Otsu-Checkpoints on a sample test image.

Table 1. Pseudo code and sample result for original otsu and otsu-checkpoints methods on image (einstein).

Otsu	
Steps	**Outcomes**
Set Range to all Gray Levels	0-255
For all t in Range: {Calculate BCV}	Bcv(0), Bcv(1), ..., Bcv(255)
Find threshold t_{max} with max BCV	t_{max}= 91

Proposed Method: Otsu-Checkpoints			
Steps	**Phase 1 (Outcomes)**	**Phase 2 (Outcomes)**	**Phase 3 (Outcomes)**
Set Search Range	0-255	77-109	85-93
Find checkpoints (cp_1, cp_2, cp_3)	77, 109, 134	85 , 93, 101	87, 89, 91
Define Sub-Ranges Formed by Checkpoint	[0-77], [77-109] [109,134], [134,255]	[77-85], [85-93] [93-101], [101,109]	[85-87], [87-89] [89-91], [91-93]
Calculate BCV for 3 Checkpoints	BCV(77), BCV(109), BCV(134)	BCV(85), BCV(93), BCV(101)	BCV(87), BCV(89), BCV(91)
Find cp_i with max BCV	$Cp_1(77)$	$Cp_2(93)$	$Cp_3(91)$
Check Bcv around selected cp(cp-1, cp, cp+1)	BCV(76) , BCV(77) , BCV(78)	BCV(92), BCV(93), Bcv(94)	BCV(90), BCV(91), BCV(92)
If Bcv at cp is Greater than BCV at (cp-1, cp+1) Then exit loop.	No	No	Yes, Exit Loop t_{max} = 91
Else Set New Range to the Sub-Range that Cover Value with max Bcv	Max Bcv at (78) New-Range [77, 109]	Max Bcv at (92) New-Range [85-93]	---
If new range is same as initial,Then exit loop	No	No	---
Else Repeat Process	Repeat Process	Repeat Process	---

Comparing Performance		
Variable/Method	**Otsu**	**Proposed**
Number of Gray Levels Checked (Iterations):	256	15
Computational Complexity:	$O(256^2)$	$O(15^2)$

5. Experimental Results

The proposed method has been implemented and evaluated using 80 real images with different dimensions and gray levels. Those test images are from Gonzalez [4], which are widely used in research papers related to image segmentation with different types of methods and techniques. First the original Otsu method (Otsu) is applied on these 80 test images; then the same images are segmented using our proposed fast Otsu method (Otsu-checkpoints) and the results are shown in Tables 2 and 3. For evaluating the performance of the proposed method against original Otsu, we have used three measures: Number of iterations, computational complexity and the estimation of accuracy. With number of iterations, we refer to the size of gray level range, which has been tested for maximum between class variance. In the conventional Otsu, this is equal to the full gray level range. The second measure is the computational complexity and it is related to the number of iterations calculating $\sigma_B^2(t)^s$. Considering the time complexity notation [3], in the conventional Otsu method, forthe full range of gray levels [0, ..., L], it requires $O(L^2)$ cycles to calculate all $\sigma_B^2(t)^s$ [2]. In our optimized Otsu method, we do not calculate $\sigma_B^2(t)^s$ for the full range of gray levels but rather this is done for a subset of gray levels. The size of this subset, denoted as Ls, is not fixed and in the worst case it will be $Ls< L/3$, thus the computational complexity will be $O(Ls^2)$. We can clearly see that the computational complexity is related to the size of the tested gray levels, which is equivalent to number of iterations. For the third measure, we have computed the accuracy of our method by estimating the threshold values by comparing the estimated threshold to that found by the original Otsu and then compute the percentage of exact matches. We have evaluated the performance of our method in enhancing the conventional Otsu by the percentages of reduction in iterations and computational complexity. The percentage of computational complexity is computed based on the assumption that for each t the computational effort for calculating $\sigma_B^2(t)^s$ is bounded by cL, where c is constant. Since, c is a constant for any value t and the computational effort is affected by the number of iterations (value of L), then the percentage of reduction can be calculated as:

$$\frac{1}{n}\cdot\sum_{i=1}^{n}(L^2 - Ls_i^2) \tag{33}$$

Where n is the number of test images.

As shown in Tables 2 and 3 (Appendix 1), our method yields excellent results, this is demonstrated by the fact that we succeeded in estimating the same threshold value found by the original Otsu method with 100% estimation accuracy, while reducing the computational complexity by an average of 99.10% and with 90.83% average reduction of the number of search iterations as shown in Table 3. As described earlier, the optimal threshold value does not always lie around the global mean; this can be clearly seen in Tables 2 and 3. For example, in 15% of the images the optimal threshold value does not occur in the area centered around the global mean. Our proposed technique has succeeded in selecting the correct area within which the exact threshold value is estimated by Otsu method. Theretofore, the results clearly show that our proposed method yields a high accuracy of threshold estimation with a significant reduction of the computational complexity when compared to original Otsu counterpart.

6. Conclusions

Digital image segmentation is an essential task in many digital image-processing applications. Obtaining better and more efficient image segmentation is a critical issue in these applications while still reducing the computational complexity. This paper has proposed a fast Otsu thresholding technique. From the evaluation of the accuracy of threshold estimation, the reduction of the computational complexity, it can be concluded that our proposed method (Otsu-checkpoints) is able to produce the same threshold value compared to the original Otsu method but with a significant reduction of the computational complexity. Thus, making it useful in many applications where real (near) real time is required.

References

[1] Alsaeed D., Bouridane A., ElZaart A., and Sammouda R., "Two Modified Otsu Image Segmentation Methods Based on Lognormal and Gamma Distribution Models," *in Proceedings of International Conference on Information Technology and e-Services (ICITeS)*, Sousse, pp. 1-5, 2012.

[2] Bazen B. and Gerez S., "Segmentation of Fingerprint Images," available at: http://citeseerx.ist.psu.edu/viewdoc/download?doi=10.1.1.122.9683&rep=rep1&type=pdf, last visited 2001.

[3] Chen L., Guo L., and Du N., "Multi-Level Image Thresholding. Based on Histogram Voting.," *in Proceedings of the 2nd International Congress on Image and Signal Processing*, Tianjin, pp. 1-5, 2009.

[4] Chen Y. and Chen O., "Image Segmentation Mehod Using Thresholds Automatically Determined From Picture Contents," *EURASIP Journal on Image and Video Processing*, vol. 2009, no. 1, pp. 1-15, 2009.

[5] Chung K. and Tsai C., "Fast Incremental Algorithm For Speeding Up The Computation Of

Binarization," *Applied Mathematics and Computation*, vol. 212, no. 2, pp. 396-408, 2009.

[6] Cormen T., Leiserson C., Rivest R., and Stein C., *Introduction to Algorithms*, MIT Press, 2009.

[7] Gonzalez R. and Woods R., *Digital Image Processing*, Prentice Hall, 2002.

[8] Li Z., Liu G., Cheng Y., Yang X., and Zhao C., "A Novel Statistical Image Thresholding Method," *AEU-International Journal of Electronics and Communications*, vol. 64, no. 12, pp. 1137-1147, 2010.

[9] Mohideen F., Niraimathi M., and Seenivasagam V., "Comparison Of Segmentation Algorithms By a Mathematical Model for Resolving Islands and Gulfs in Nuclei of Cervical Cell Images," *The International Arab Journal of Information Technology*, vol. 12, no. 5, pp. 424-430, 2015.

[10] Narayana C., Reddy E., and Prasad M., "Article: Automatic Image Segmentation Using Ultra Fuzziness," *International Journal of Computer Applications*, vol. 49, no. 12, pp. 6-13, 2012.

[11] O'Gorman L., "Experimental Comparisons of Binarization and Multithresholding Methods on Document Images," *in Proceedings of the 12th IAPR International Conference on Pattern Recognition, Conference B*: *Computer Vision and Image Processing*, Jerusalem, pp. 395-398, 1994.

[12] Otsu N., "A Threshold Selection Method from Gray-level Histograms," *IEEE Transactions on Systems, Man and Cybernetics*, vol. 9, no. 1, pp. 62-66, 1979.

[13] Pham D., Xu C., and Prince J., "A Survey of Current Methods in Medical Image Segmentation," *in Proceedings of Annual Review of Biomedical Engineering*, pp. 318-338, 2000.

[14] Raut S., Raghuvanshi M., Dharaskar R., and Raut A., "Image Segmentation A State-Of-Art Survey for Prediction," *in Proceedings of International Conference on Advanced Computer Control*, Singapore, pp. 420-424, 2009.

[15] Sezgin M. and Sankur B., "Survey Over Image Thresholding Techniques and Quantitative Performance Evaluation," *Journal of Electronic Imaging*, vol. 13, no. 1, pp. 146-168, 2004.

[16] Wan Y., Wang J., Sun X., and Hao M., "A Modified Otsu Image Segment Method Based On the Rayleigh Distribution," *in Proceedings of the 3rd IEEE International Conference on Computer Science and Information Technology*, Chengdu, pp. 281-285, 2010.

[17] Xu L., Jackowski M., Goshtasby A., Roseman D., Bines S., Yu C., Dhawan A., and Huntley A., "Segmentation of Skin Cancer Images," *Image and Vision Computing*, vol. 17, no. 1, pp. 65-74, 1999.

[18] Zhang J. and Hu J., "Image Segmentation Based On 2d Otsu Method with Histogram Analysis," *in Proceedings of International Conference on Computer Science and Software Engineering*, pp. 105-108, 2008.

Duaa Alsaeed received a BCS degree in computer science in 1992 and an M.Phil. degree in computer science (image processing) in 2005; both degrees from the College of Computer and Information Sciences (CCIS), King Saud University, Saudi Arabia. She is now studying for a PhD in computer science (image processing) in the Department of Computer Science and Digital Technologies at Northumbria University, UK. From 1993 to 2005, she worked as a teacher of computer courses for high school students with hearing disabilities in the Ministry of Education, Saudi Arabia. From 2005-2008 she worked as a general educational supervisor for special education in the Ministry of Education, Saudi Arabia. In 2008, she worked as a general technical and educational supervisor in the Technical and Vocational Training Corporation; in 2009, she joined King Saud University as a lecturer in the College of Computer and Information Sciences (CCIS), and her research interests are in image processing and imagesegmentation.

Ahmed Bouridane received an "Ingenieurd'Etat" degree in electronics from "Ecole Nationale Polytechnique" of Algiers (ENPA), Algeria, in 1982, an M.Phil. degree in electrical engineering (VLSI design for signal processing) from the University of Newcastle-Upon-Tyne, U.K., in 1988, and an Ph.D. degree in electrical engineering (computer vision) from the University of Nottingham, U.K., in 1992. From 1992 to 1994, he worked as a Research Developer in telesurveillance and access control applications. In 1994, he joined Queen's University Belfast, Belfast, U.K., initially as Lecturer in computer architecture and image processing and later on he was promoted to Reader in Computer Science. He is now a full Professor in Image Engineering and Security and leads the Computer and Electronic Security Systems Group at Northumbria University at Newcastle (UK), and his research interests are in imaging for forensics and security, biometrics, homeland security, image/video watermarking, cryptography and mobile and visual computing. He has authored and co-authored more than 250 publications and one research book. he is a Senior Member of IEEE.

Ali El-Zaart was a senior software developer at Department of Research and Development, Semiconductor Insight, Ottawa, Canada during 2000-2001. From 2001 to 2004, he was an assistant professor at the Department of Biomedical Technology, College of Applied Medical Sciences. From 2004 to April 2010, he was an assistant professor at the Department of Computer Science, College of computer and information Sciences. Since April 2010, he is an associate professor at the same department. Presently he is an associate professor at the Beirut Arab University. He has published numerous articles and proceedings in the areas of image processing, remote sensing, and computer vision. He received a BSc in computer science from the University of Lebanon; Beirut, Lebanon in 1990, M.Sc. degree in computer science from the University of Sherbrooke, Sherbrooke, Canada in 1996, and Ph.D. degree in computer science from the University of Sherbrooke, Sherbrooke, Canada in 2001. His research interests include image processing, pattern recognition, remote sensing, and computer vision.

Appendix 1

Table 2. Estimated thresholds and evaluation for methods: Otsu, proposed otsu-checkpoints (part-1).

Image	Threshold		Global	Checkpoints			Selected	No. of	%	%
	Otsu	Proposed	Mean	Cp_1	Cp_2	Cp_3	Cp	Itrs	Itrred	Cmplxred
Chickenfilet with Bones	79	79	94	80	85	90	1	15	94.14	99.66
Einstein	90	90	109	87	89	91	3	15	94.14	99.66
MRI of Knee Univ Mich	121	121	142	121	122	123	2	25	90.23	99.05
MRI Spine1 Vandy	108	108	68	108	109	110	2	25	90.23	99.05
Skin Cancer 19	98	98	117	99	101	103	1	15	94.14	99.66
Skin Cancer 4	112	112	124	113	114	115	1	20	92.19	99.39
Skin Cancer 5	91	91	99	88	90	92	3	15	94.14	99.66
Skin Cancer 7	74	74	94	75	76	77	1	20	92.19	99.39
Skin Cancer 8	91	91	95	91	92	93	2	20	92.19	99.39
Skin Cancer 9	74	74	78	74	75	76	2	20	92.19	99.39
Washingtondc Band4	133	133	147	134	135	136	1	38	85.16	97.80
Bacteria	98	98	96	97	99	101	2	15	94.14	99.66
Blob Original	108	108	121	109	110	111	1	28	89.06	98.80
Blobs	170	170	119	170	171	172	2	25	90.23	99.05
Blobs In Circular Arrangement	142	142	156	143	145	147	1	20	92.19	99.39
Boats	105	105	141	104	105	106	3	20	92.19	99.39
Brain	46	46	49	43	45	47	3	15	94.14	99.66
Brain Tomur (1)	77	77	50	78	84	90	1	15	94.14	99.66
Brain Tomur (2)	69	69	50	70	72	74	1	20	92.19	99.39
Brain Tomur (3)	59	59	31	60	61	62	1	20	92.19	99.39
Brain Tomur (4)	81	81	30	74	78	82	3	15	94.14	99.66
Bubbles	174	174	140	175	181	187	1	15	94.14	99.66
Building Original	146	146	134	147	148	149	1	38	85.16	97.80
Cameraman	88	88	120	89	91	93	1	20	92.19	99.39
Chest Xray Vandy	103	103	143	100	102	104	3	20	92.19	99.39
Columbia	100	100	82	99	100	101	3	20	92.19	99.39
Crabpulsar Optical	131	131	104	132	133	134	1	33	87.11	98.34
Ctskull 256	117	117	130	118	119	120	1	28	89.06	98.80
Cygnusloop Xray Original	75	75	68	75	76	77	2	25	90.23	99.05
Dark Blobs on Light Background	142	142	155	142	143	144	2	25	90.23	99.05
Defective Weld	167	167	174	168	169	170	1	38	85.16	97.80
Dental Xray	146	146	168	146	147	148	2	20	92.19	99.39
Face	80	80	94	81	82	83	1	20	92.19	99.39
Fb1	132	132	137	133	134	135	1	33	87.11	98.34
Fb10	176	176	209	177	182	187	1	15	94.14	99.66
Fb11	181	181	216	180	181	182	3	20	92.19	99.39
Fb12	130	130	132	131	132	133	1	33	87.11	98.34
Fb13	148	148	175	149	150	151	1	38	85.16	97.80
Fb14	152	152	171	152	153	154	2	20	92.19	99.39
Fb15	150	150	183	149	151	153	2	20	92.19	99.39
Fb16	112	112	113	113	114	115	1	33	87.11	98.34
Fb17	110	110	99	111	113	115	1	20	92.19	99.39
Fb18	159	159	175	160	161	162	1	20	92.19	99.39
Fb19	125	125	141	125	126	127	2	25	90.23	99.05
Fb2	181	181	211	182	183	184	1	33	87.11	98.34
Fb20	153	153	144	153	154	155	2	20	92.19	99.39
Fb3	160	160	181	161	162	163	1	33	87.11	98.34
Fb4	149	149	165	150	151	152	1	38	85.16	97.80
Fb5	105	105	74	105	106	107	2	25	90.23	99.05
Fb6	147	147	166	146	147	148	3	20	92.19	99.39
Fb7	128	128	134	128	129	130	2	25	90.23	99.05
Fb8	142	142	160	143	144	145	1	33	87.11	98.34
Fb9	174	174	203	174	175	176	2	20	92.19	99.39
Headct Vandy	90	90	81	91	92	93	1	33	87.11	98.34
House	117	117	109	117	118	119	2	20	92.19	99.39
Contd. In Tabel 3										

Table 3. Estimated thresholds and evaluation for methods: Otsu, proposed otsu-checkpoints (part-2).

Image	Threshold		Global	Checkpoints			Selected	No. of	%	%
	Otsu	Proposed	Mean	Cp_1	Cp_2	Cp_3	Cp	Itrs	ItrRed	Cmplxred
Kidney	127	127	116	128	129	130	1	33	87.11	98.34
Large Septagon	118	118	111	115	119	123	2	15	94.14	99.66
Left Hand Xray	79	79	52	79	80	81	2	20	92.19	99.39
Lena	101	101	107	101	102	103	2	20	92.19	99.39
Lung	85	85	81	86	88	90	1	20	92.19	99.39
Noisy Region	181	181	147	182	183	184	1	20	92.19	99.39
Ordered Matches	143	143	114	139	144	149	2	15	94.14	99.66
Orig Chest Xray	78	78	61	79	80	81	1	33	87.11	98.34
Polymersomes	181	181	171	181	182	183	2	25	90.23	99.05
Radar1	42	42	28	43	44	45	1	33	87.11	98.34
Radar2	65	65	47	56	66	76	2	10	96.09	99.85
Radar3	52	52	57	43	48	53	3	10	96.09	99.85
Random Matches	143	143	111	143	144	145	2	25	90.23	99.05
Rice Image with Intensity Gradient	134	134	117	134	135	136	2	20	92.19	99.39
Scalp	52	52	52	52	53	54	2	20	92.19	99.39
Skull	96	96	36	96	97	98	2	25	90.23	99.05
Small Blobs Original	120	120	131	121	122	123	1	33	87.11	98.34
Third from Top	111	111	114	112	113	114	1	28	89.06	98.80
Tooth	109	109	147	109	110	111	2	25	90.23	99.05
Tungsten Filament Shaded	75	75	94	68	72	76	3	15	94.14	99.66
Tungsten Original	99	99	129	88	94	100	3	15	94.14	99.66
Turbine Blade Black Dot	132	132	135	133	134	135	1	28	89.06	98.80
Weld Original	167	167	174	168	169	170	1	38	85.16	97.80
Wood Dowels	121	121	88	122	123	124	1	33	87.11	98.34
Yeast USC	42	42	34	42	43	44	2	20	92.19	99.39
Evaluation of Performance Among all Experiments (Tables 1, 2) For Proposed Method (Otsu-Checkpoints)										
Accuracy = 100% **Percentage of Reduction in:** **1. No. Of Checked Gray Values = 90.83%** **2. Computational Complexity = 99.10%**										